

Dynamical heterogeneity in the Ising spin glass

Sharon C. Glotzer,¹ Naeem Jan,² Turab Lookman,³ Allan B. MacIsaac,³ and Peter H. Poole³

¹*Polymers Division and Center for Theoretical and Computational Materials Science,
National Institute of Standards and Technology, Gaithersburg, Maryland 20899*

²*Department of Physics, St. Francis Xavier University, Antigonish, Nova Scotia, Canada B2G 2W5*

³*Department of Applied Mathematics, University of Western Ontario, London, Ontario, Canada N6A 5B7*

(Received 8 October 1997)

We investigate the relationship between bulk and local relaxation in the Ising spin glass (in two and three dimensions) for temperatures above but approaching the glass transition temperature, using Monte Carlo computer simulations. We find that the stretched exponential form of the bulk spin autocorrelation function results from a spatial average over a broad range of behavior, from strongly nonexponential to nearly exponential, for the local autocorrelation functions. The spatial correlation of single-site relaxation times obtained from these functions provides a length scale for dynamical heterogeneity that grows with decreasing temperature. [S1063-651X(98)10806-1]

PACS number(s): 64.70.Pf, 75.50.Lk, 75.10.Nr

As a disordered system is cooled toward a glass transition, equilibrium relaxation functions decay in a complex way. In liquids with self-induced frustration [1] and in spin glasses with quenched disorder [2,3], the density autocorrelation function and spin autocorrelation function, respectively, decay nonexponentially. These autocorrelation functions are well approximated for large time t by a stretched exponential or Kohlrausch-Williams-Watts function $\exp(-t/\tau)^\beta$, where τ and β are temperature-dependent fit parameters.

The relationship of this bulk late-time behavior to relaxation at a local, microscopic level is not understood. A widely debated open question concerns whether individual microscopic regions of a glass-forming system relax ‘‘homogeneously’’ or ‘‘heterogeneously’’ above the glass transition temperature [1,4,5]. In the homogeneous scenario, an autocorrelation function of a microscopic region of the system decays as a stretched exponential and all microscopic regions decay similarly with the same values of τ and β as for the bulk behavior. In one widely discussed heterogeneous scenario, autocorrelation functions for different microscopic regions decay as simple exponentials but with different values of τ , the average of these local exponential relaxations yielding the observed stretched exponential behavior of the bulk.

A model system for which this question is readily addressed is the $\pm J$ Ising spin glass [2]. For this system, the disorder is quenched and it is therefore expected that local relaxation will vary as a function of position, i.e., dynamical heterogeneity will occur. This has been confirmed for short-time-scale dynamics through the observation of spatial variations in the equilibrium spin-flip rates for $T > T_{SG}$ [6]. However, a detailed characterization of long-time local relaxation, required to elucidate the behavior of the bulk relaxation function, has not been reported. Furthermore, it should be possible in the Ising spin glass to explicitly measure a length scale for dynamical heterogeneity, that is, a length scale over which the local spin relaxation is spatially correlated. This quantity is currently of great interest to the glass community [1,4,5]. Here we evaluate and characterize the range of functional behavior for local relaxation in the

Ising spin glass. We thereby elucidate the relationship between bulk and local relaxation and identify a length scale for dynamical heterogeneity.

We perform simulations of the Ising spin glass in dimensions $d=2$ and 3 in the paramagnetic phase at temperatures T above the spin-glass transition temperature T_{SG} . The system is described by the Hamiltonian $H = -\sum_{\langle ij \rangle} s_i J_{ij} s_j$, on a square ($d=2$) or simple cubic ($d=3$) lattice. In our simulations the external magnetic field is zero. Exchange interactions $J_{ij} = \pm J$ are randomly assigned to the edges of the lattice and Ising spins $s_i = \pm 1$ are placed on each site i . The sum in H is taken over all nearest-neighbor pairs of sites. We use the heat-bath Monte Carlo algorithm [7] with periodic boundary conditions for lattices of size 64^2 ($d=2$) and 16^3 ($d=3$). Our simulations are performed for several values of kT/J . In $d=2$, $kT/J=1.6, 1.8$ and 2.0 ; in $d=3$, $kT/J=2.5, 3.0$, and 3.5 . Since $kT_{SG}/J=0$ and 1.175 ± 0.025 in $d=2$ and 3, respectively [2], all simulations are performed well above T_{SG} [8].

We calculate the local equilibrium spin autocorrelation function $q_i(t)$ for each site i , which for the paramagnetic phase can be defined as $q_i(t) = \langle s_i(0)s_i(t) \rangle$ [3]. Here angular brackets indicate an average over choices of the time origin $t=0$. The number of sites in our lattices for both $d=2$ and 3 is $N=64^2=16^3=4096$ and hence for each T simulated we obtain a set $\{q_i(t)\}$ of 4096 functions. Each $q_i(t)$ is evaluated from $t=0$ to $t=t_{\max}$, where t_{\max} is chosen so that $q_i(t_{\max}) < 0.01$ for all i , that is, we determine all $q_i(t)$ over at least two decades of decay. The value of t_{\max} increases as T decreases. It is consequently an appropriate parameter for choosing run times for the equilibration and production phases of each simulation since by definition within this time *all* sites become (essentially) uncorrelated from their state at earlier t . For equilibration, we carry out at least $10^3 t_{\max}$ Monte Carlo steps (MCS). To evaluate all $q_i(t)$ functions to within an accuracy of ± 0.01 , a production phase of at least $6 \times 10^4 t_{\max}$ MCS is required. At the lowest T studied $t_{\max} \approx 500$ MCS, leading to run times of at least 3×10^7 MCS.

It is convenient to characterize local relaxation in terms of $q_i(t)$ because the bulk autocorrelation function $q(t)$ conven-

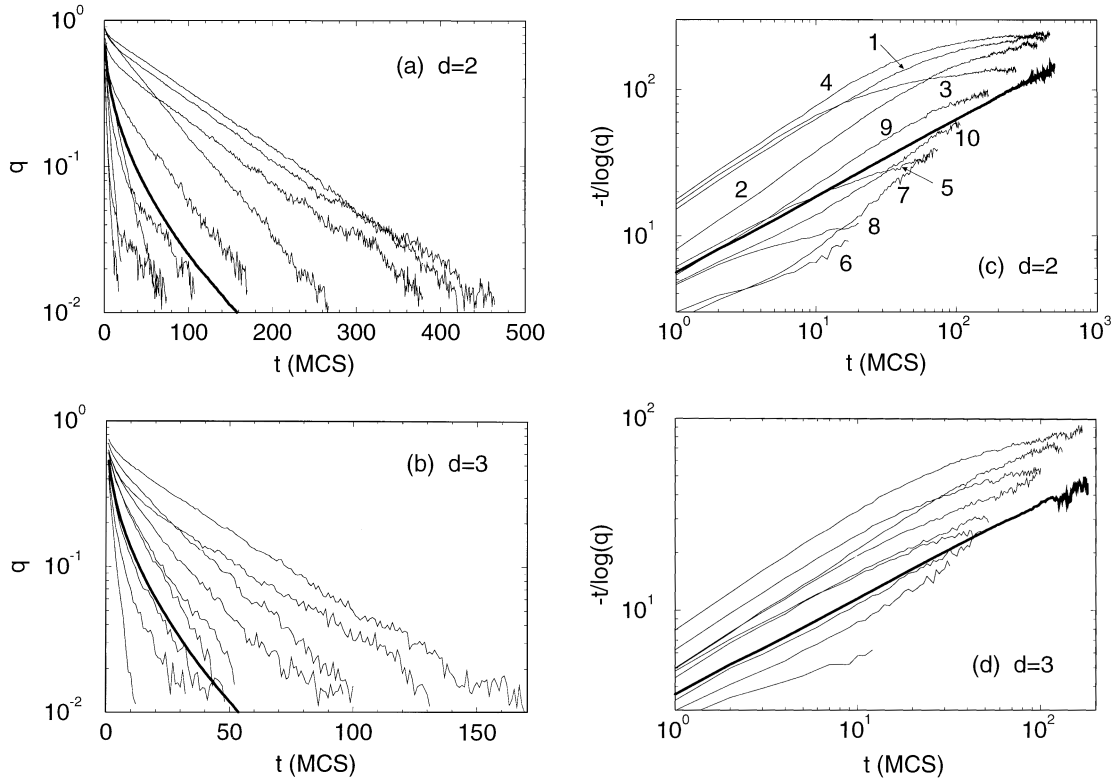


FIG. 1. Plots of $q_i(t)$ (thin lines) for several spins in $d=2$ for $kT/J=1.6$ [(a) and (c)], and $d=3$ for $kT/J=2.5$ [(b) and (d)]. The bulk function $q(t)$ (heavy line) is also shown. (a) and (b) are semilogarithmic plots versus t . In (c) and (d) the same data are shown in a log-log plot of $-t/\log(q)$ versus t . All logarithms are base 10. The locations of the sites for the $q_i(t)$ curves given in (c) are indicated in Fig. 4(b) by \circ 's with the corresponding number.

tionally studied for the Ising spin glass is evaluated by averaging over all $q_i(t)$ functions: $q(t) = N^{-1} \sum_{i=1}^N q_i(t)$ [3,9]. Our results for $q(t)$ for $d=3$ agree with those of Ref. [3], where it was shown that a product of algebraic and stretched exponential functions

$$q(t) \approx ct^{-x} \exp(-t/\tau)^\beta \quad (1)$$

fits well to $q(t)$. c , x , τ and β are T -dependent fit parameters. Depending on T , it has been found that $x \in (0, 0.5)$ and $\beta \in (0.3, 1.0)$, while τ diverges as $T \rightarrow T_{SG}$ [3].

Figure 1 shows $q_i(t)$ for several different i , representative of the range of behavior we observe. Also shown for comparison is $q(t)$. The dynamical heterogeneity expected for the Ising spin glass is apparent: For both $d=2$ and 3 there is a broad range of behavior among the $q_i(t)$ curves, with some decaying much more rapidly than the average and some much less.

To test if the $q_i(t)$ functions, like $q(t)$, follow the form of Eq. (1), we carry out an exhaustive nonlinear least-squares fit of Eq. (1) to $q_i(t)$ for all sites. We find that Eq. (1) fits well to each $q_i(t)$ over the two decades of decay studied here. We also find that a broad spectrum of both τ and β values results from the fits (Fig. 2). Hence, if the local relaxation in both $d=2$ and 3 is analyzed in terms of Eq. (1) over the first two decades of decay, then the stretched exponential relaxation of the bulk does not result from a superposition of simple exponential local relaxations. Rather, we find that the Ising spin glass in this time regime is spatially heterogeneous with respect to both the τ and β parameters in Eq. (1) [10].

Note also from Fig. 2 that most of the β values obtained at one value of T occur in the range from 0.3 to 1.0. In Ref. [3], when Eq. (1) was fit to $q(t)$ for many different $T > T_{SG}$, although β was found to vary through the same range, τ increased and β decreased as T decreased. This correlation is reversed in the case of $q_i(t)$: For a given T , τ tends to decrease as β decreases. Hence, at the level of individual sites at fixed T , slow relaxation is *less* “stretched” than fast relaxation.

The data from Figs. 1(a) and 1(b) are plotted in Figs. 1(c) and 1(d) so that exponential relaxation gives a horizontal line, while stretched exponential relaxation yields a straight line with nonzero slope. Despite the fact that both $q(t)$ and several $q_i(t)$ display stretched exponential behavior, the

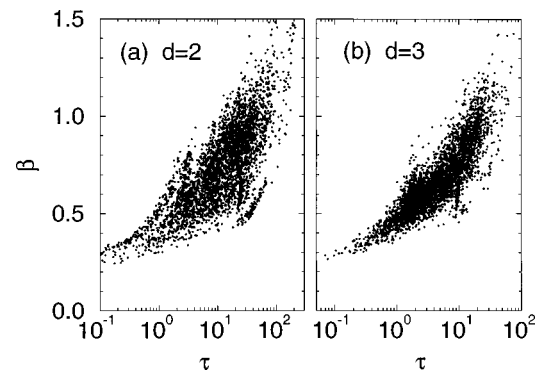


FIG. 2. Scatter plots of the fit parameters τ and β for all sites for (a) $d=2$ ($kT/J=1.6$) and (b) $d=3$ ($kT/J=2.5$).

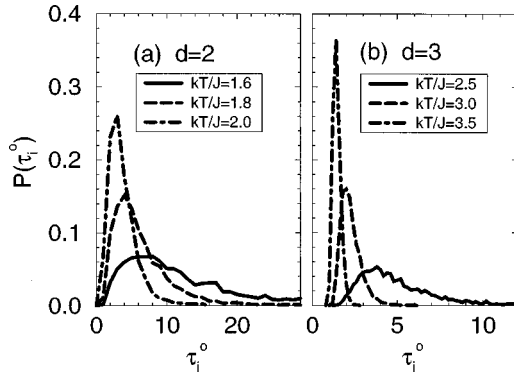


FIG. 3. $P(\tau_i^0)$ versus τ_i^0 for various T in (a) $d=2$ and (b) $d=3$.

other $q_i(t)$, specifically the most slowly decaying, appear at large t to be approaching exponential behavior, consistent with the implications of Fig. 2. This observation raises several possibilities.

(i) The observation of nearly exponential relaxation at the local level supports the possibility, raised in earlier studies [11,12], that there exist localized regions of the system that relax independently in the range of T studied here (the ‘‘Griffiths phase’’).

(ii) There may exist a regime of t in which a significant

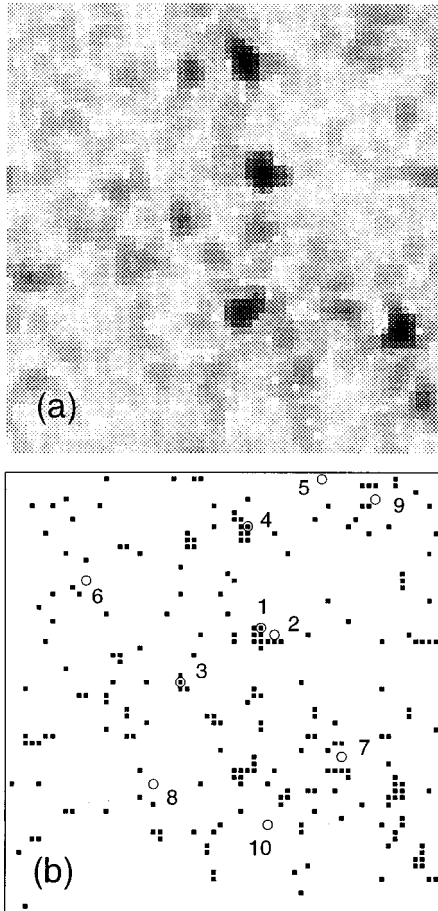


FIG. 4. (a) Spatial arrangement of τ_i^0 values in $d=2$ for $kT/J=1.6$. Large values of τ_i^0 are shown in black, small values in white. (b) Locations of unfrustrated sites (■) and sites (numbered ○'s) for which $q_i(t)$ is plotted in Fig. 1(c).

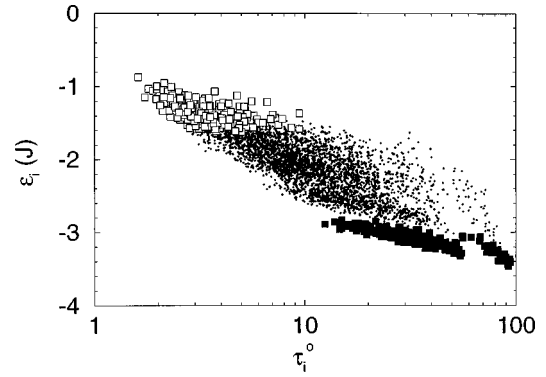


FIG. 5. Scatter plot of ϵ_i versus τ_i^0 for all sites for $d=2$ and $kT/J=1.6$. Points are shown for unfrustrated sites (■) frustrated sites (□) and all other sites (●).

contribution to the stretched exponential bulk relaxation arises from a sum of simple exponential functions, each associated with a localized region of the system and each with a different characteristic relaxation time [1,4].

(iii) If the slowest relaxing site in the range of t studied here (shown as the topmost curves in Fig. 1) remains the slowest as $t \rightarrow \infty$, then it will impose an upper bound on the asymptotic functional behavior of $q(t)$ [9,12,13]. If $q_i(t)$ for this site is asymptotically exponential, then $q(t)$ will cross over from stretched to simple exponential relaxation as $t \rightarrow \infty$. Conversely, the slowest relaxing site on the time scale monitored here may not be slowest as $t \rightarrow \infty$, in which case other sites, perhaps with nonexponential relaxation functions, may dominate the asymptotic bulk relaxation. Our data would have to be extended over several more decades of t to confirm which of these possibilities is most likely. Regardless of the outcome, our results show that specific scenarios for asymptotic bulk relaxation can be developed from a study of local relaxation, even on a time scale in which the bulk behavior is far from its asymptotic regime.

Finally, we test for the existence of a characteristic length scale for dynamical heterogeneity. To this end, we study the distribution and spatial arrangement of local relaxation times. Since Eq. (1) presently lacks rigorous physical justification, rather than using τ , we choose a generic (and easier to evaluate) local relaxation time τ_i^0 defined as the zeroth moment of the corresponding $q_i(t)$ function, $\tau_i^0 \equiv \int_0^\infty q_i(t) dt$ [14]. We calculate τ_i^0 by numerically integrating the data for $q_i(t)$ from $t=0$ to t_{\max} . The distribution of τ_i^0 values for

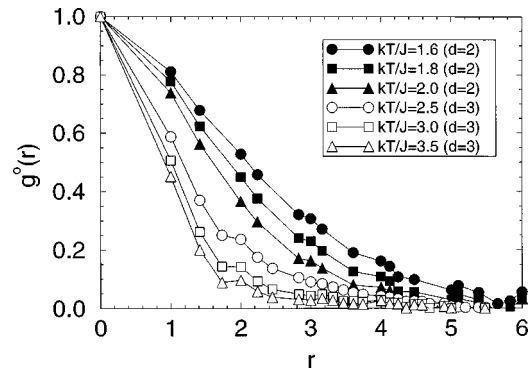


FIG. 6. $g^0(r)$ versus r for various T in $d=2$ and $d=3$.

three different $T > T_{SG}$ in both $d=2$ and 3 is shown in Fig. 3. As T decreases these distributions broaden dramatically and display an increasingly pronounced tail to large τ_i^0 , similar to behavior found recently for local energy and flip rate distributions [6,15].

The spatial arrangement of τ_i^0 values at $kT/J=1.6$ in $d=2$ is shown in Fig. 4(a). The largest values of τ_i^0 are spatially correlated and their locations correspond well to contiguous groups of unfrustrated sites [Fig. 4(b)] [16]. This correlation is also demonstrated in Fig. 5: unfrustrated sites have both lower energy ϵ_i and larger τ_i^0 than the average, while frustrated sites have higher ϵ_i and smaller τ_i^0 [17]. Hence Fig. 4 approximately images the clusters of the Griffiths phase [11].

To quantify the spatial correlation of the set $\{\tau_i^0\}$, we calculate the correlation function $g^0(r)$ obtained by averaging over sites i and j separated by the same distance r , the

quantity $(\langle \tau_i^0 \tau_j^0 \rangle - \langle \tau_i^0 \rangle \langle \tau_j^0 \rangle) / [\langle (\tau_i^0)^2 \rangle - \langle \tau_i^0 \rangle^2]$. Here angular brackets denote an average over all sites in the system. Figure 6 shows $g^0(r)$ for different $T > T_{SG}$. As T decreases, $g^0(r)$ decays more slowly as a function of r , demonstrating that the length scale associated with dynamical heterogeneity is growing as T decreases. It would be interesting to determine if this dynamically defined length approaches a finite value as $T \rightarrow T_{SG}$ or if it is related to the growth and eventual divergence of the conventional static correlation length. The result may indicate how to use these dynamically correlated regions to formulate a cluster description of the Ising spin glass transition [18,19].

We thank K. Binder, J.P. Bouchaud, R.V. Chamberlain, A. Coniglio, G. Parisi, H. Rieger and D. Stauffer for useful discussions. N.J., T.L., A.B.M., and P.H.P. acknowledge the support of NSERC (Canada). S.C.G. and N.J. thank the Center for Chemical Physics (UWO) for their hospitality.

-
- [1] M. D. Ediger, C. A. Angell, and S. R. Nagel, *J. Phys. Chem.* **100**, 13 200 (1996).
- [2] K. Binder and A. P. Young, *Rev. Mod. Phys.* **58**, 801 (1986); H. Rieger, *Annual Reviews of Computational Physics* (World Scientific, Singapore, 1995), Vol. 2, p. 295; K. H. Fischer and J. A. Hertz, *Spin Glasses* (Cambridge University Press, Cambridge, 1991).
- [3] A. T. Ogielski, *Phys. Rev. B* **32**, 7384 (1985).
- [4] R. Richert, *Chem. Phys.* **122**, 455 (1988); K. Schmidt-Rohr and H. W. Spiess, *Phys. Rev. Lett.* **66**, 3020 (1991); R. V. Chamberlain and D. W. Kingsbury, *J. Non-Cryst. Solids* **172-174**, 318 (1994); H. Heuer *et al.*, *Phys. Rev. Lett.* **75**, 2851 (1995); R. Richert, *J. Phys. Chem. B* **101**, 6323 (1997).
- [5] W. Kob, C. Donati, S.J. Plimpton, P. H. Poole, and S. C. Glotzer, *Phys. Rev. Lett.* **79**, 2827 (1997); C. Donati, J.F. Douglas, W. Kob, S.J. Plimpton, P.H. Poole, and S.C. Glotzer, *ibid.* **80**, 2338 (1998).
- [6] P. H. Poole, S. C. Glotzer, A. Coniglio, and N. Jan, *Phys. Rev. Lett.* **78**, 3394 (1997).
- [7] K. Binder, in *Monte Carlo Methods in Statistical Physics*, edited by K. Binder (Springer-Verlag, Berlin, 1986); B. Derrida and G. Weisbuch, *Europhys. Lett.* **4**, 657 (1987).
- [8] Our results are obtained for one particular random $\{J_{ij}\}$ configuration for the quenched disorder, the same as that used in Ref. [6]. Simulations using different configurations confirm that our conclusions are not affected by the choice of $\{J_{ij}\}$.
- [9] K. Hukushima and K. Nemoto, *J. Phys. Soc. Jpn.* **64**, 2183 (1995).
- [10] The exponent x also takes on a range of values between 0 and 0.5. However, we restrict our attention to τ and β in this work since the stretched exponential character of Eq. (1) is of widest interest.
- [11] R. B. Griffiths, *Phys. Rev. Lett.* **23**, 17 (1969).
- [12] M. Randeria, J. P. Sethna, and R. G. Palmer, *Phys. Rev. Lett.* **54**, 1321 (1985).
- [13] A. T. Ogielski, *Phys. Rev. B* **36**, 7315 (1987).
- [14] The results reported here using τ_i^0 are qualitatively unchanged if we use instead the values of τ obtained from fitting the $q_i(t)$ curves to Eq. (1).
- [15] Note that the flip rate ν_i evaluated in Ref. [6] characterizes the short-time behavior of $q_i(t)$. Specifically, $\nu_i = [1 - q_i(1)]/2$.
- [16] An elementary plaquette of a square or simple cubic lattice is termed unfrustrated (frustrated) if the product of the J_{ij} values for the four edges of the plaquette is $+1$ (-1). We define an unfrustrated (frustrated) site as a site for which all of the neighboring elementary plaquettes are unfrustrated (frustrated).
- [17] ϵ_i is defined as the time average of $-\sum_j s_i J_{ij} s_j$, where j labels the nearest-neighbor sites of i ; see Ref. [6].
- [18] A. Coniglio, in *Correlations and Connectivity*, edited by H. E. Stanley and N. Ostrowsky (Kluwer, Dordrecht, 1990).
- [19] S. C. Glotzer and A. Coniglio, *Comput. Mater. Sci.* **4**, 325 (1995).